

Local Patterns Generalize Better for Novel Anomalies

Yalong Jiang, Liquan Mao
Beihang University, Beijing 100191, China
AllenYLJiang@outlook.com

Abstract. Video anomaly detection (VAD) aims at identifying novel actions or events which are unseen during training. Existing mainstream VAD techniques focus on the global patterns of events and cannot properly generalize to novel samples. In this paper, we propose a framework to identify the spatial local patterns which generalize to novel samples and model the dynamics of local patterns. In spatial part of the framework, the capability of extracting local patterns is gained from image-text contrastive learning with Image-Text Alignment Module (ITAM). To detect different types of anomalies, a two-branch framework is proposed for representing the local patterns in both actions and appearances. In temporal part of the framework, a State Machine Module (SMM) is proposed to model the dynamics of local patterns by decomposing their temporal variations into motion components. Different dynamics are represented with different weighted sums of a fixed set of motion components. The video sequences with either novel spatial distributions of local patterns or distinctive dynamics of local patterns are deemed as anomalies. Extensive experiments on popular benchmark datasets demonstrate that state-of-the-art performance can be achieved.

Keywords: Global Patterns; Local Patterns; Image-Text Alignment Module; State Machine Module; Motion Components

1. Introduction

Video anomaly detection (VAD) is the task of localizing from videos the events that do not match regular patterns, such as violence, accidents and other unexpected events. Nowadays, numerous platforms such as CCTVs and UAVs play an increasingly important role in surveillance. However, it is infeasible for humans to pinpoint anomalies in such an enormous amount of data among which the probability of abnormal events' existence approaches zero. Besides, the domain difference between anomalous events and normal ones leads to lack in prior knowledge about anomalies. As a result, VAD is a hot topic in weakly supervised or unsupervised learning [2,10,28,30,55,61,69,78,84,112].

Existing main-stream works [28, 43, 58] for VAD are divided into three categories. The first type of methods detect the anomalies with distinctive spatial and temporal features. Two widely used examples are prediction-based [55, 58, 61, 70] and reconstruction-based [12, 52, 62, 103] approaches. To address the issue of limited model representational capacity caused by limited training data, other methods propose to combine various feature clues [14, 28], including skeletal

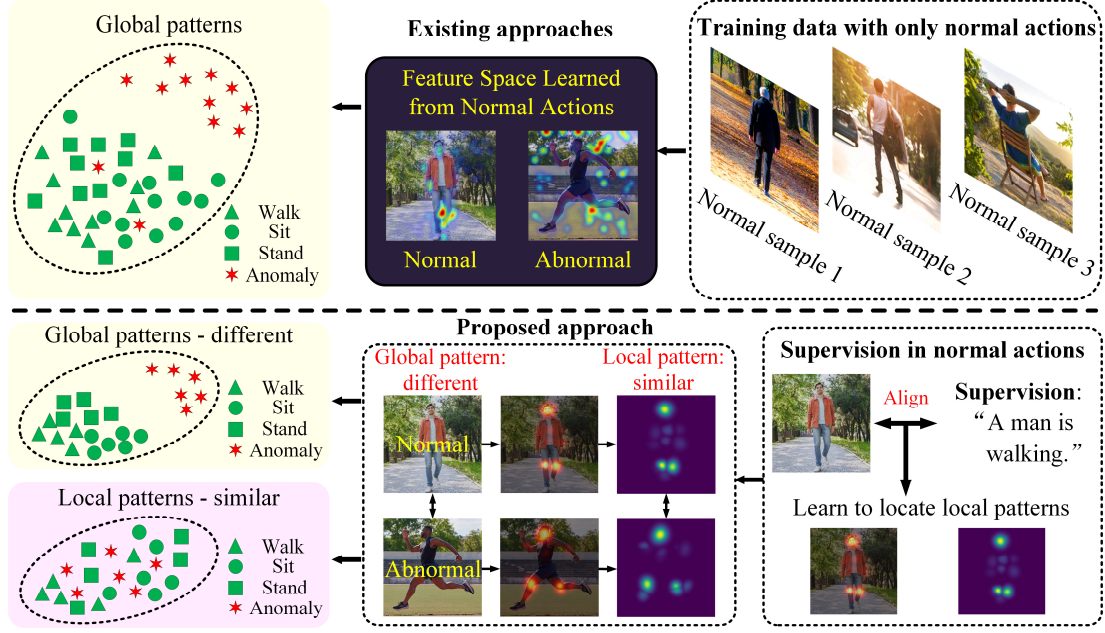


Fig. 1: Top: Existing representations with global patterns cannot generalize to novel samples. Normal and abnormal samples are not well distinguished. Bottom: Image-text alignment empowers the model to find the local patterns which generalize to novel samples, the divergences in local patterns' spatial distributions determine anomalies.

trajectories, appearance, motion patterns, moving directions and casual reasoning [51]. The second type of approaches apply multiple instance learning (MIL) to iterate between finding useful segments for model fine-tuning and fine-tuning models [14, 38, 53, 94, 124], using dynamic clustering to adapt models' representations to real-time observations [97, 104]. The feature spaces of some of the above approaches cannot well generalize to novel abnormal events, as is shown by Fig. 1. The third type of approaches [53] attempt to generate realistic anomalies to facilitate the construction of decision boundary between normal and abnormal samples. However, the generated anomalies are based on prior assumptions and still differ from real anomalous samples.

Target at generalizing model representations to novel anomalies, we introduce Image-Text Alignment Module (ITAM) which empowers the proposed framework to find local patterns through aligning captions with visual elements during training. As is shown by Fig. 1, different from global patterns which are sensitive to contextual variations, ITAM enforces the proposed framework to extract the local patterns that generalize to different events and are applicable to novel samples. The divergences in local patterns' spatial arrangements and dynamics facilitate the measurements of similarities across seen and unseen samples.

In sum, the proposed framework is composed of a spatial part and a temporal part. The spatial part consists of two branches: Branch 1 for learning action-related local patterns, and Branch 2 which encodes the patterns of object appearances. The temporal part is introduced to represent the dynamics in spatial local patterns with a common set of motion components. Abnormal actions and objects are distinguished with respect to spatial and temporal patterns. The effectiveness of the framework is validated on six benchmarks, i.e., ShanghaiTech, Avenue and so on. The

contributions of this paper can be highlighted as follows:

- This paper proposes to gain from image-text alignment the capability to capture the local patterns which generalize to novel abnormal samples. The samples with abnormally distributed local patterns or anomalous dynamics are considered to be anomalies.
- The proposed framework is prediction based. It is composed of a spatial part for identifying local patterns and a temporal part for modeling the dynamics of local patterns through making predictions. Anomalous videos produce increased prediction error.
- State-of-the-art performance is achieved with the proposed framework on multiple benchmark datasets.

2. Related Work

2.1. Unsupervised Video Anomaly Detection

Due to the imbalanced nature of surveillance videos, most available training datasets are without anomaly annotations because it is expensive to label [17, 42, 50]. Reconstruction-based approaches [1, 6, 24, 30, 41, 79, 103] produce increased error when encountering irregular spatio-temporal features [75] that do not reside in training data. For instance, [64, 108] improved model structures for better reconstruction. [27, 30] augmented encoders to improve the sensitivity of reconstruction error to anomalies. [12, 63, 85, 107] integrated appearances, motion features, audio features and rule-based features [19]. [34] reconstructed images with a probabilistic decision model. [111] distinguished good and bad quality reconstructions to improve stability. Prediction-based methods such as [48, 58, 59, 66, 67, 114] evaluated the divergence in normal and abnormal temporal dependencies, leveraging latent spaces [118] or hybrid attention [117].

To better distinguish anomalies under ambiguous cases, [52, 55, 61, 70] combined prediction with reconstruction and built a pool of features for encoding normal dynamics. [60, 81, 98] studied the distribution over normal patterns and proposed novel deep features [4] to separate anomalies from normal samples. Similarly, [101] proposed denoising diffusion modules to learn the distribution of normal events. [26] exploited the enhanced mode coverage capabilities of diffusive probabilistic models. To distinguish anomalous patterns with better representations, [101] proposed contrastive and snippet-level anomalous attention. [26] introduced pyramid deformation module and localization mechanism to enhance the power of reconstruction. [72] leveraged CRFs to learn the dependencies across frames. To fully exploit task-relevant features, [86] combined interpolation with extrapolation for prediction. [95] proposed a self-supervised learning scheme with discriminative DNNs. [83] proposed to sequentially learn multiple pretext tasks to enhance anomaly detection. Although remarkable improvements have been achieved, some of the representations cannot well represent unseen abnormal patterns. We propose to describe out-of-domain anomalies with generalizable patterns.

2.2. Weakly Supervised Anomaly Detection

Multi-instance learning (MIL) takes videos as bags and snippets as instances, transforming video-level labels to instance-level supervision [25]. The methods iteratively locate abnormal segments and fine-tune models using the segments. To collect abnormal segments, inter-sample similarities are evaluated [35, 56]. For instance, clustering-based approaches measured the similarity in spatio-temporal embeddings [12, 18, 62, 65]. [] proposed a probabilistic framework for categorizing actions. [89] built graphical representations connecting different objects. [14] integrated collective properties in measuring similarities. Then the anomalous segments which are dissimilar to normal ones [115] function in fine-tuning. [80] performed dynamic non-parametric clustering and exposed the model to potentially positive instances. To improve robustness and efficiency, [119] proposed to interpret the vulnerability of MIL. [99] introduced casual relations to enhance MIL [91]. [102] proposed binary network augmentation strategy to improve detection performance. Differently, we propose generalizable representations which bridge the gap between normal and abnormal events, facilitating the measurement of similarities between normal and novel events.

2.3. Methods with Data Augmentation

To generate pseudo abnormal samples as supervision in fine-tuning models, methods such as [7, 36, 46, 47, 53] proposed pseudo abnormal snippet synthesizers which are trained on normal samples [105]. [110] employed a generator which was not fully trained to create abnormal samples as supervision. [13] proposed to generate class balanced supplementary training data with a conditional GAN. [45] focused on infrequent normal samples during generation, harnessing novel sampling strategies. Besides frame-level analysis [112], human-level approaches [35, 58, 90] provide more fine-grained analysis. Similarly, [20] identified the outliers as positive samples by assigning anomaly scores to objects. [3] introduces a new dataset with diverse anomalies. However, the generated samples are based on normal patterns and still differ from real-world anomalies.

2.4. Methods Exploring the Representation of Unseen Categories

To adapt model representations and work under changing anomalies, meta learning-based methods such as [55, 70], transfer-learning based approaches [20, 71] and self-supervised approaches [16, 69] introduced adjustable feature representations to adapt to new domains. Attention-based methods such as [32, 40, 57, 87, 88] attended to domain-invariant features in addressing unseen samples while reducing background influences. To better align with anomaly detection, [28] integrated multiple sub-tasks, including moving direction prediction, appearance consistency evaluation and object classification. [123] introduced multi-level graphs for representing videos and maximizing the margins between normal and abnormal ones. Differently, our proposed approach locates the local patterns which generalize to unseen categories of events. The patterns are learned from image-text alignment. Besides spatial patterns, the dynamics of local patterns are modeled with state machines [31] which are embedded with motion components.

2.5. Prompting Methods

Prompt-based approaches have been widely used in anomaly detection [22, 53, 53, 81]. Different from the approaches which leverage complex backbones, the proposed approach combines a

Resnet-18 based backbone with an image-text alignment module for obtaining language-informative local patterns.

3. Our Method

Targeted at representing both normal and unexpected abnormal events using generalizable representations, we establish a framework capable of identifying local patterns. The framework includes a spatial part and a temporal part which jointly determine anomalies. In the following sections, we will first introduce the structure of the proposed framework and then elaborate on the techniques that empower the model to locate local patterns.

3.1. Structure of the Framework

In order to detect the anomalies manifested by different objects, object detection is conducted, as is shown in Fig. 2. Specifically, we adopt the Region Proposal Network (RPN) in [121] which generalizes to the objects with unknown categories. Considering the fact that interactions exist between neighboring objects, we combine each bounding box with its neighbors which share overlapping regions before feeding the combined box into the framework. For instance, a human and a neighboring bicycle are combined. For a single object which does not overlap with others, we crop a squared region with side length being equal to its longest side.

To identify local patterns in different objects, the spatial part of the framework consists of Branch 1 and Branch 2 for representing human actions and objects' appearances, respectively.

Denote $\mathbf{v}_{i,1}(t) \in \mathbb{R}^{N_q E_d}$ and $\mathbf{v}_{i,2}(t) \in \mathbb{R}^{N_q E_d}$ the outputs from both branches. $\mathbf{v}_{i,1}(t)$ and $\mathbf{v}_{i,2}(t)$ are

combined to $\mathbf{v}_i(t) \in \mathbb{R}^{N_q E_d}$ which describes Bounding Box i at t . The contributions of an additional branch [74] which describes background contexts will be illustrated in ablation studies.

The temporal part of the framework learns to predict $\mathbf{v}_i(t+1)$ based on $\mathbf{v}_i(t-L+1), \dots, \mathbf{v}_i(t)$.

Sequences with abnormal dynamics produce higher prediction error. We create a tube with length $L=5$ by cropping the same bounding box region from L frames. To account for fast moving objects, we enlarge bounding boxes by 25% along both dimensions prior to creating tube.

3.2. Spatial Part of the Proposed Framework

To identify local patterns, the spatial part firstly extracts visual features with backbones and then locates local patterns based on visual features. The capability of locating patterns is gained by performing image-text alignment with ITAM. In Branch b $b \in (1,2)$ in Fig. 2, one backbone

network firstly maps input B_s images to visual features $H_{i,b}^I(t) \in \mathbb{R}^{S_d \times V_d}$. S_d denotes the number of spatial elements in embeddings while V_d denotes the dimension of visual representations. ITAM includes an Image-attention Module for extracting language-informative local patterns from $H_{i,b}^I(t)$ and a Text-attention Module for textual features. ITAM learns to align the features from

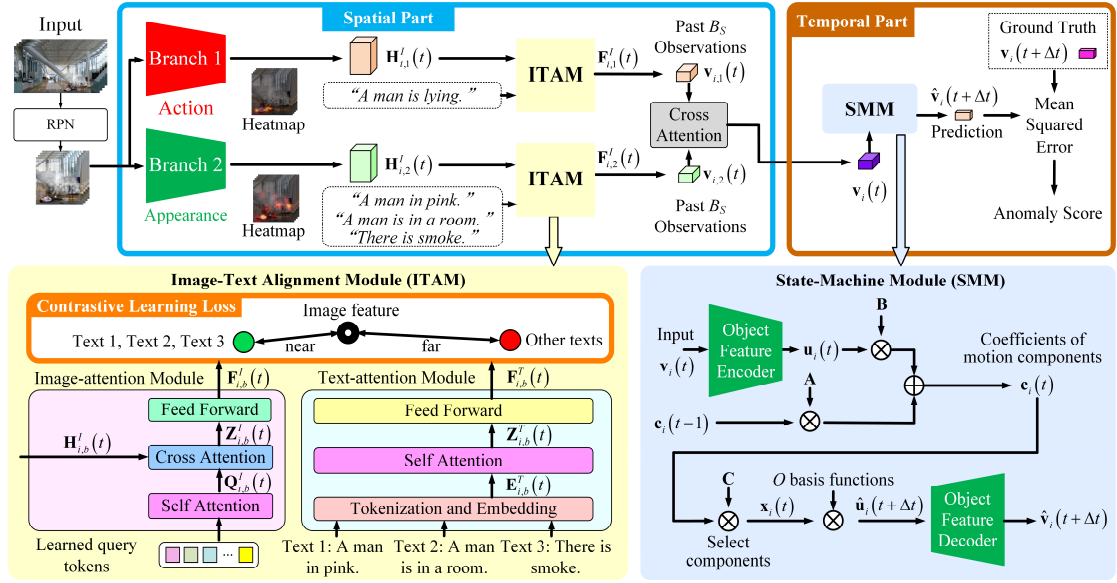


Fig. 2: Structure of the proposed framework which is divided into a spatial part for finding local patterns and a temporal part for modeling the dynamics of local patterns. The spatial part includes two branches each of which consists of a backbone and an Image-Text Alignment Module (ITAM). In ITAM, an Image-attention Module and a Text-attention Module extract visual and textual features before aligning them. The outputs from both branches are combined to obtain the local patterns representing inputs. In temporal part of the framework, a State Machine Module (SMM) is proposed to model the dynamics of local patterns by learning to make predictions.

Image-attention Module and Text-attention Module. In inference, the output $F'_{i,b}(t) \in \mathbb{R}^{N_q \times E_d}$ from

Image-attention Module produces $v_{i,b}(t) \in \mathbb{R}^{B_s \times N}$ with $N = N_q E_d$.

Backbone In Branch 1, a resnet-18 based structure is adopted as backbone which is trained together with ITAM in an end-to-end fashion. To provide fine-grained spatial features, we keep the output from the 8-th layer in resnet-18 with shape $28 \times 28 \times 512$. Branch 2 shares the same structure as Branch 1 but differs in training labels. In each branch, the backbone and ITAM are trained together from scratch on the anomaly detection datasets with only normal samples.

Image-attention Module in ITAM To extract from visual features the caption-informative local patterns, this module is built with self-attention layers, cross-attention layers and feed-forward layers, as is shown by Fig. 2. Firstly, N_q learnable query embeddings representing different features are fed into self-attention layers before interacting with $H'_{i,b}(t)$ through

cross-attention layers. The queries have shape $N_q \times H_d$ where $N_q = 32$ denotes the number of queries and $H_d = 768$ is embedding size. The self-attention layers are implemented according to [93] and has output $Q'_{i,b}(t) \in \mathbb{R}^{N_q \times H_d}$. The cross attention layers perform feature fusion by

combining $H'_{i,b}(t)$ with $Q'_{i,b}(t)$ to $Z'_{i,b}(t) \in \mathbb{R}^{N_q \times H_d}$ which are projected by fully-connected feed

forward layers to $F'_{i,b}(t) \in \mathbb{R}^{N_q \times E_d}$.

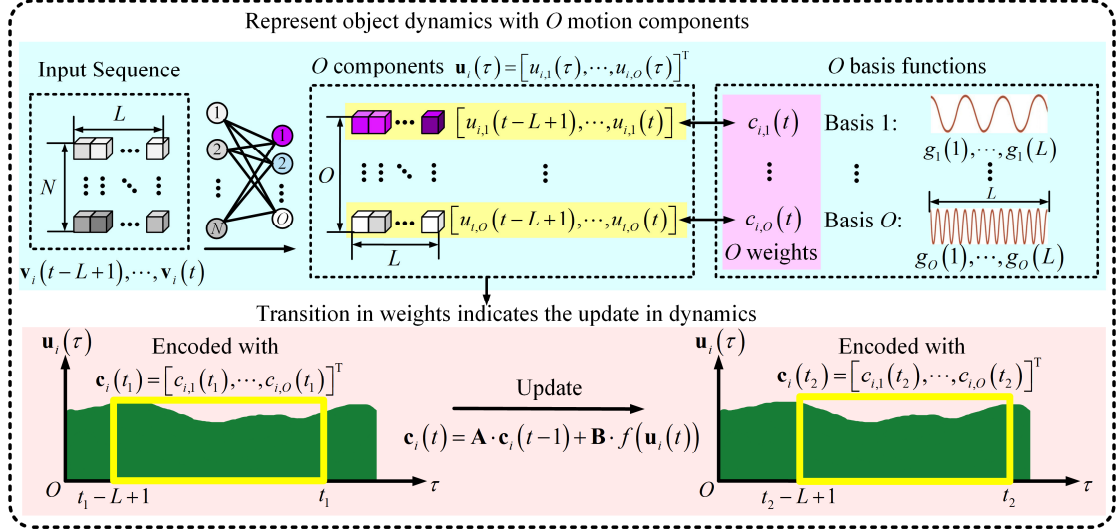


Fig. 3: SMM leverages O motion components in representing the dynamics of local patterns across L frames. The N -dimensional dynamics are encoded with O weights which correspond to the components.

Text-attention Module in ITAM To extract textual features, the module is built with embedding layers, self-attention layers and feed-forward layers, as is shown by Fig. 2. The features of N_s sentences which correspond to the same image are extracted together. In the example of Branch 2 in Fig. 2, $N_s = 3$. Firstly, the input tensor with N_s sentences are tokenized and input to embedding layer which produces $E_{i,b}^T(t) \in \mathbb{R}^{N_s \times S_l \times H_d}$ where S_l denotes maximum sequence length. Then the self-attention layers project $E_{i,b}^T(t) \in \mathbb{R}^{N_s \times S_l \times H_d}$ to $Z_{i,b}^T(t) \in \mathbb{R}^{N_s \times S_l \times H_d}$ which undergoes dimension reduction and produces $Z_{i,b}^T(t) \in \mathbb{R}^{N_s \times H_d}$. Finally, the feed-forward layers produce $F_{i,b}^T(t) \in \mathbb{R}^{N_s \times E_d}$.

In ITAM, both Image-attention Module and Text-attention Module are used for training while only Image-attention Module is kept in inference.

Loss function for Image-Text Contrastive Learning ITAM learns to align the visual local patterns $F_{i,b}^I(t)$ with textual features $F_{i,b}^T(t)$. It achieves this goal by contrasting the image-text similarity of a positive pair against those of negative pairs within the same batch of size B_s . As is shown by Fig. 2 where the same image is fed into both branches, the captions for training Branch 1 is "A man is lying" while those for training Branch 2 include "A man in pink", "A man is in a room" and "There are smokes". In the example of Branch 2, the image is more similar to the last three sentences than other sentences.

$F_{i,b}^T(t)$ is allocated to N_s groups. Each group involves B_s sentences and only one ground truth. Cross entropy loss is computed to make sure the similarity between an image and its ground truth sentence in one group exceeds those between the image and other sentences. The loss function is:

$$L_{ITAM} = -\frac{1}{2N_s B_s} \sum_{n=0}^{N_s-1} \left(\sum_{i=0}^{B_s-1} \sum_{c=0}^{B_s-1} y_{n,i,c} \log(\hat{y}_{n,i,c}) + \sum_{c=0}^{B_s-1} \sum_{i=0}^{B_s-1} w_{n,c,i} \log(\hat{w}_{n,c,i}) \right) \quad (1)$$

where $\mathbf{y}_{n,i} \in \mathbb{R}^{B_s}$ is a one-hot vector. In the n -th group where each image is matched with B_s sentences, $\mathbf{y}_{n,i,c}$ takes 1 only when the i -th image is better matched with the c -th sentence than others. Similarly, $\mathbf{w}_{n,c,i}$ takes 1 only when the c -th sentence is better matched with the i -th image than others.

In the computation of image-text similarity, the cosine similarity between all of the N_q queries in $F_{i,b}^I(t)$ and $F_{i,b}^T(t)$ are computed with the maximum one kept, N_q queries represent different features of the same image and the one which is most informative about captions is kept.

The sentences for training are generated with CLIP model [74] with an image encoder and a text encoder. For each image region, we generate four sentences which describe the subject's action, appearance, background and nearby objects, respectively. The word embedding which has highest cosine similarity with a visual vector from CLIP image encoder is selected, and inserted into a template such as "A man is doing something", "A man is in some clothes", "A man is in some place" and "There is something". Specifically, we select from Oxford-3000 vocabulary [92] the words describing actions, clothes, places and objects. For non-human objects, we also select verbs for training the first branch.

3.3. Temporal Part of the Proposed Framework

To model the dynamics of different objects using fixed motion components $[g_o(1), \dots, g_o(L)]$, $o \in [1, O]$ which are O length- L Legendre polynomials [5], SMM is proposed and is shown in Fig. 2 and Fig. 3. Specifically, the input tensor $[\mathbf{v}_i(t-L+1), \dots, \mathbf{v}_i(t)] \in \mathbb{R}^{N \times L}$ is projected to the weighted versions of O fixed motion components. The projection is achieved with the Object Feature Encoder in Fig. 2, producing $[\mathbf{u}_i(t-L+1), \dots, \mathbf{u}_i(t)] \in \mathbb{R}^{O \times L}$ with $\mathbf{u}_i(\tau) = [u_{i,1}(\tau), \dots, u_{i,O}(\tau)]^T$.

$$u_{i,o}(\tau) = c_{i,o}(t) g_o(\tau - t + L), o \in [1, O], \tau \in [t-L+1, t] \quad (2)$$

In SMM, a state vector $\mathbf{c}_i(t) \in \mathbb{R}^O$ with O weights $c_{i,1}(t), \dots, c_{i,O}(t)$ encodes an object's dynamics through L moments, each weight corresponds to one Legendre basis function. The transitions in weights indicate the updates in objects' dynamics. As O grows, more diversified basis functions enable the generalization to more dynamics. At each moment, the new-coming $\mathbf{v}_i(t)$ updates the O weights which show the importance of motion components.

$$\mathbf{c}_i(t) = \mathbf{A} \mathbf{c}_i(t-1) + \mathbf{B} \sum_{o=1}^O u_{i,o}(t) \quad (3)$$

where $\mathbf{A} = \mathbf{A}_{\text{Legendre}}(O, L) \in \mathbb{R}^{O \times O}$ and $\mathbf{B} = \mathbf{B}_{\text{Legendre}}(O, L) \in \mathbb{R}^{O \times 1}$ are determined by Legendre bases according to [31]. $\mathbf{c}_i(t-1)$ encodes $[\mathbf{u}_i(t-L), \dots, \mathbf{u}_i(t-1)]$ while $\mathbf{c}_i(t)$ encodes $[\mathbf{u}_i(t-L+1), \dots, \mathbf{u}_i(t)]$. The derivation of Eq. (3) will be included in supplementary materials.

SMM learns to predict future states by selecting the motion components which account for normal temporal variations. The prediction error on abnormal sequences grows because the selected bases cannot explain for abnormal actions. In the proposed approach, learnable matrix $\mathbf{C} \in \mathbb{R}^{O \times O}$ is proposed to highlight the components that correspond to normal dynamics:

$$\mathbf{x}_i(t) = \mathbf{C}\mathbf{c}_i(t) \quad (4)$$

By combining Eq. (3) with Eq. (4), we obtain

$$\mathbf{x}_i(t) = \mathbf{C}\mathbf{A}^{L-1}\mathbf{B}\sum_{o=1}^O u_{i,o}(t-L+1) + \dots + \mathbf{C}\mathbf{A}\mathbf{B}\sum_{o=1}^O u_{i,o}(t-1) + \mathbf{C}\mathbf{B}\sum_{o=1}^O u_{i,o}(t) \quad (5)$$

Finally, the elements of $\mathbf{x}_i(t)$ are multiplied with shifted motion components

$[g_o(1+\Delta t), \dots, g_o(L+\Delta t)], o \in [1, O]$, producing the shifted versions of weighted motion components:

$$\hat{u}_{i,o}(\tau + \Delta t) = x_{i,o}(t)g_o(\tau - t + L + \Delta t) \quad (6)$$

The Object Feature Decoder projects $\hat{\mathbf{u}}_i(t + \Delta t) = [\hat{u}_{i,1}(t + \Delta t), \dots, \hat{u}_{i,O}(t + \Delta t)]^T$ to the predicted visual features in future moments $\hat{\mathbf{v}}_i(t + \Delta t) = [\hat{v}_{i,1}(t + \Delta t), \dots, \hat{v}_{i,O}(t + \Delta t)]^T$, as is shown by Fig. 2.

4. Experiments

4.1. Dataset and Metric

To demonstrate the effectiveness of the proposed framework, we conduct experiments on datasets: ShanghaiTech [48], CUHK Avenue [54]. The training sets of ShanghaiTech, Avenue and UCSD Ped2 contain only normal events and abnormal behaviors reside in test data.

ShanghaiTech dataset contains 330 training videos and 107 test videos with 130 abnormal events. Typical anomalies include fighting, running, cycling and so on. Among the two versions of ShanghaiTech dataset [48] and [38, 120], the latter [113, 124] includes abnormal behaviors in both training set and test set. As our approach is unsupervised, we use the first version. HR-ShanghaiTech includes only human-related video, six non-human test videos are neglected [33].

CUHK Avenue dataset involves 16 and 21 video clips for training and test, respectively. The dataset covers abnormal movements and moving directions. In HR-Avenue, non-human anomalies are ignored [66].

Evaluation Metrics Following previous literatures [65], Area under Curve (AUC, %) is adopted for evaluation, it is computed by continuously changing the threshold for anomaly detection before conducting integration. A higher AUC value indicates better performance.

Different from other datasets, the accuracy on XD-Violence dataset is measured by precision-recall curve and the corresponding Average Precision (AP, %) [68].

4.2. Implementation Details

As is shown by Fig. 2, an off-the-shelf Region Proposal Network (RPN) [77] is leveraged. For each detected object, if it is overlapped with neighboring bounding boxes, then we merge it with neighbors. If the merged bounding box is not squared, we enlarge its regions along the short side to include more background contexts. Each bounding box is resized to 224×224 before being fed into backbones. The output from backbone $H_{i,b}^I(t) \in \mathbb{R}^{S_d \times V_d}$ is projected by the Image-attention

Module in ITAM to $F_{i,b}^I(t) \in \mathbb{R}^{N_q \times E_d}$ which is the output of the spatial part of the framework.

$S_d = 257$, $V_d = 1408$, $N_q = 32$, $E_d = 256$. The detailed structures will be illustrated in supplementary materials.

The backbones in Branch 1 and Branch 2 have Resnet-18 structures with only first two stages kept, producing a $28 \times 28 \times 512$ tensor for each image. The tensor is resized to $16 \times 16 \times 1408$. Class token [21] with size V_d for each input image is concatenated with backbones' resized outputs, producing $H_{i,b}^I(t) \in \mathbb{R}^{S_d \times V_d}$. Branch 1 and Branch 2 are trained independently. We firstly train the

spatial part to extract features $\mathbf{v}_i(t)$, then freeze the spatial part and train SMM to predict future features based on past ones.

Hyperparameters for training Spatial Part The learning rate schedule is Linear Warmup With Cosine Annealing. The warmup learning rate is 10^{-6} which increases to initial learning rate 10^{-4} and then decreases to minimum learning rate 10^{-5} in a cosine annealing learning rate schedule. The warmup stage lasts for 5000 steps. The batch size for training is 120.

Hyperparameters for training Temporal Part The learnable weights in SMM include those in the Object Feature Encoder (OFE) with $N_q E_d$ input channels and $O=64$ output channels and

those in Object Feature Decoder (OFD) with O input channels and $N_q E_d$ output channels. The

OFE and OFD are linear layers. Besides, the weights in $C \in \mathbb{R}^{O \times O}$ are learnable. All weights are initialized according to distribution $N(0, 0.02)$. Training lasts for 20 epoches, initial learning rate is 5×10^{-5} with learning rate decay 0.99. The cross attention layer for combining the outputs from branches is trained together with SMM.

Implementations are based on Pytorch platform [73]. Experiments are conducted on one NVIDIA A100 GPU. On the datasets [88, 100, 3] where training data includes anomalies, the procedures for training the spatial part of the framework remain the same. For instance, CLIP model [74] is also leveraged in generating labels. The spatial part learns to produce different spatial arrangements of local patterns in different events. The temporal part of the framework only learns on the training videos without anomalies.

4.3. Comparisons with Related Methods

Table 1: Performance (AUC, %) on the ShanghaiTech, CUHK Avenue, Ubnormal and UCSD Ped2. Micro-AUC [76] is evaluated.

Algorithm	Year	ShanghaiTech	CUHK Avenue
Georgescu et al. [29]		82.7	90.4
Wang et al. [96]		76.6	88.3
Li et al. [37]	2021	73.9	88.8
Acsintoae et al. [2]		-	-
Bertasius et al. [8]		-	-
Reiss et al. [76]		85.9	93.3
Zaheer et al. [109]		79.6	74.2
Cho et al. [15]		76.3	88.0
Zhong et al. [122]	2022	74.5	89.0
Wang et al. [94]		84.3	92.2
Yang et al. [104]		74.7	89.9
Zhang et al. [116]		80.3	80.5
Liu et al. [53]		85.0	93.6
Cao et al. [9]		79.2	86.8
Yang et al. [103]		73.8	89.9
Hirschorn et al. [33]		85.9	-
Arad et al. [4]	2023	85.9	93.5
Acsintoae et al. [3]		83.7	93.0
Sun et al. [90]		83.4	93.7
Liu et al. [49]		78.8	92.8
Yu et al. [106]		72.6	90.7
Ours	2024	88.6	93.7

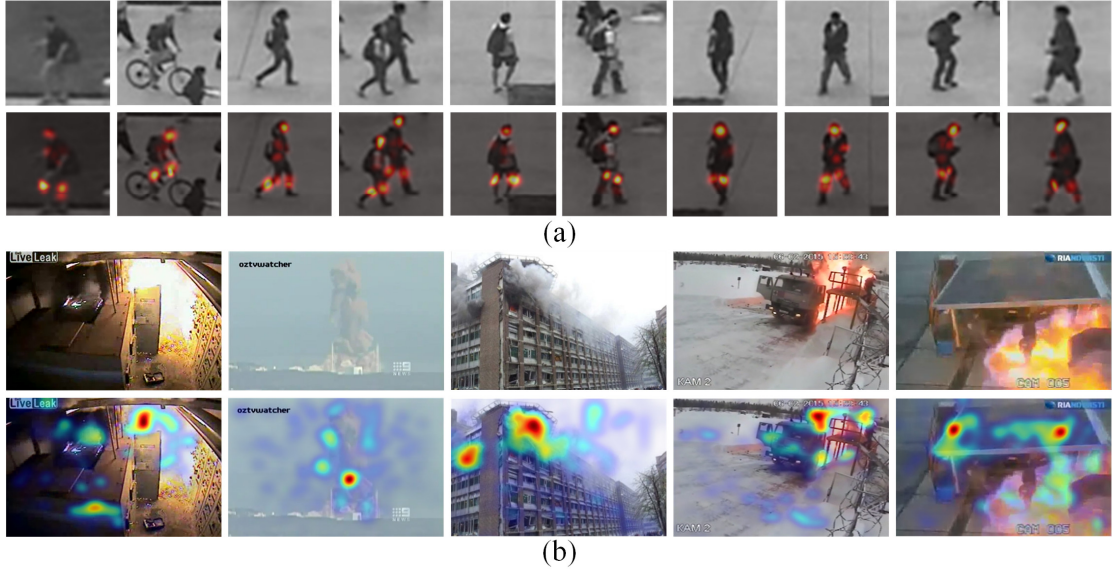


Fig. 4: Heatmaps of local patterns. (a) Low-resolution humans. (b) Abnormal objects whose spatial distributions of local patterns differ from those of normal objects.

The proposed approach is compared with existing ones in detecting different types of anomalies, as is shown in Table 1. Then the effectiveness is verified on different types of objects.

4.4. Subjective Results

The local patterns in low-resolution videos can also be located. Example data are from UCSD Ped2 dataset where the resolution of a single human is about 30×30 pixels. It can be seen from Fig. 4 that local patterns can be accurately located regardless of low resolutions. The heatmaps are obtained with [82] based on the data in $H_{i,b}^l(t)$.

5. Conclusion

In this paper, we establish a framework for video anomaly detection by locating visual local patterns and modeling the dynamics of local patterns. At the core of the framework is to identify the local patterns which can generalize to novel anomalies. In this way, anomalies can be detected by the distinctive spatial and temporal arrangements of local patterns which reside in normal and abnormal events. The framework includes a spatial part and a temporal part. The former consists of a backbone and an ITAM, and learns to identify local patterns. The temporal part models the dynamics of local patterns with motion components. Extensive experiments on six benchmarks show that the framework surpasses existing state-of-the-art methods, demonstrating that image-text contrastive learning empowers the model to locate generalizable local patterns. In the future, we will try to enhance the efficiency of the framework.

References

1. Abati, D., Porrello, A., Calderara, S., Cucchiara, R.: Latent space autoregression for novelty detection. In: Proceedings of the IEEE/CVF Conference on Computer Vision and Pattern Recognition. pp. 481–490. IEEE (2019)
2. Acsintoae, A., Florescu, A., Georgescu, M.I., Mare, T., Sumedrea, P., Ionescu, R.T., Khan, F.S., Shah, M.: Ubnormal: New benchmark for supervised open-set video anomaly detection. arXiv preprint arXiv:2111.08644 (2021)
3. Acsintoae, A., Florescu, A., Georgescu, M.I., Mare, T., Sumedrea, P., Ionescu, R.T., Khan, F.S., Shah, M.: Ubnormal: New benchmark for supervised open-set video anomaly detection. In: Proceedings of the IEEE/CVF Conference on Computer Vision and Pattern Recognition. pp. 20143–20153 (2022)
4. Arad, Y., Werman, M.: Beyond the benchmark: Detecting diverse anomalies in videos. arXiv preprint arXiv:2310.01904 (2023)
5. Arfken, G.B., Weber, H.J., Harris, F.E.: Mathematical methods for physicists: a comprehensive guide. Academic press (2011)
6. Asad, M., Yang, J., Tu, E., Chen, L., He, X.: Anomaly3d: Video anomaly detection based on 3d-normality clusters. Journal of Visual Communication and Image Representation 75, 103047 (2021)
7. Astrid, M., Zaheer, M.Z., Lee, S.I.: Synthetic temporal anomaly guided end-to-end video anomaly detection. In: Proceedings of the IEEE/CVF International Conference on Computer Vision. pp. 207–214 (2021)
8. Bertasius, G., Wang, H., Torresani, L.: Is space-time attention all you need for video understanding? In: ICML. vol. 2, p. 4 (2021)
9. Cao, C., Lu, Y., Wang, P., Zhang, Y.: A new comprehensive benchmark for semi-supervised video anomaly detection and anticipation. In: Proceedings of the IEEE/CVF Conference on Computer Vision and Pattern Recognition. pp. 20392–20401 (2023)
10. Chalapathy, R., Menon, A.K., Chawla, S.: Robust, deep and inductive anomaly detection. In: Proceedings of the Joint European Conference on Machine Learning and Knowledge Discovery in Databases. pp. 36–51. Springer (2017)
11. Chang, S., Li, Y., Shen, S., Feng, J., Zhou, Z.: Contrastive attention for video anomaly detection. IEEE Transactions on Multimedia 24, 4067–4076 (2021)
12. Chang, Y., Tu, Z., Xie, W., Yuan, J.: Clustering driven deep autoencoder for video anomaly detection. In: European Conference on Computer Vision. pp. 329–345. Springer (2020)
13. Chen, Z., Duan, J., Kang, L., Qiu, G.: Supervised anomaly detection via conditional generative adversarial network and ensemble active learning. IEEE Transactions on Pattern Analysis and Machine Intelligence 45(6), 7781–7798 (2022)
14. Cho, M., Kim, M., Hwang, S., Park, C., Lee, K., Lee, S.: Look around for anomalies: Weakly-supervised anomaly detection via context-motion relational learning. In: Proceedings of the IEEE/CVF Conference on Computer Vision and Pattern Recognition. pp. 12137–12146 (2023)
15. Cho, M., Kim, T., Kim, W.J., Cho, S., Lee, S.: Unsupervised video anomaly detection via normalizing flows with implicit latent features. Pattern Recognition 129, 108703 (2022)
16. Degardin, B., Proença, H.: Iterative weak/self-supervised classification framework for

- abnormal events detection. *Pattern Recognition Letters* 145, 50–57 (2021)
17. Deng, A., Yang, T., Chen, C.: A large-scale study of spatiotemporal representation learning with a new benchmark on action recognition pp. 20519–20531 (2023)
 18. Dhiman, C., Vishwakarma, D.K.: View-invariant deep architecture for human action recognition using two-stream motion and shape temporal dynamics. *IEEE Transactions on Image Processing* 29, 3835–3844 (2020)
 19. Ding, M., Chen, Z., Du, T., Luo, P., Tenenbaum, J., Gan, C.: Dynamic visual reasoning by learning differentiable physics models from video and language. In: *Advances in Neural Information Processing Systems*. vol. 34 (2021)
 20. Doshi, K., Yilmaz, Y.: Continual learning for anomaly detection in surveillance videos. In: *Proceedings of the IEEE/CVF Conference on Computer Vision and Pattern Recognition Workshops*. pp. 254–255 (2020)
 21. Dosovitskiy, A., Beyer, L., Kolesnikov, A., Weissenborn, D., Zhai, X., Unterthiner, T., Dehghani, M., Minderer, M., Heigold, G., Gelly, S., et al.: An image is worth 16x16 words: Transformers for image recognition at scale. *arXiv preprint arXiv:2010.11929* (2020)
 22. Du, Y., Wei, F., Zhang, Z., Shi, M., Gao, Y., Li, G.: Learning to prompt for open-vocabulary object detection with vision-language model. In: *Proceedings of the IEEE/CVF Conference on Computer Vision and Pattern Recognition*. pp. 14084–14093 (2022)
 23. Fan, Y., Yu, Y., Lu, W., Han, Y.: Weakly-supervised video anomaly detection with snippet anomalous attention. *IEEE Transactions on Circuits and Systems for Video Technology* (2024)
 24. Fang, Z., Zhou, J.T., Xiao, Y., Li, Y., Yang, F.: Multi-encoder towards effective anomaly detection in videos. *IEEE Transactions on Multimedia* 23, 4106–4116 (2020)
 25. Feng, J.C., Hong, F.T., Zheng, W.S.: Mist: Multiple instance self-training frame-work for video anomaly detection. In: *Proceedings of the IEEE/CVF conference on computer vision and pattern recognition*. pp. 14009–14018 (2021)
 26. Flaborea, A., Collorone, L., Di Melendugno, G.M.D., D’Arrigo, S., Prenkaj, B., Galasso, F.: Multimodal motion conditioned diffusion model for skeleton-based video anomaly detection. In: *Proceedings of the IEEE/CVF International Conference on Computer Vision*. pp. 10318–10329 (2023)
 27. Gao, J., Zhong, B., Chen, Y.: Robust tracking via learning model update with unsupervised anomaly detection philosophy. *IEEE Transactions on Circuits and Systems for Video Technology* (2022)
 28. Georgescu, M.I., Barbalau, A., Ionescu, R.T., Khan, F.S., Popescu, M., Shah, M.: Anomaly detection in video via self-supervised and multi-task learning. In: *Proceedings of the IEEE/CVF Conference on Computer Vision and Pattern Recognition*. pp. 12742–12752. IEEE (2021)
 29. Georgescu, M.I., Ionescu, R.T., Khan, F.S., Popescu, M., Shah, M.: A background-agnostic framework with adversarial training for abnormal event detection in video. *IEEE transactions on pattern analysis and machine intelligence* 44(9), 4505–4523 (2021)
 30. Gong, D., Liu, L., Le, V., Saha, B., Mansour, M., Venkatesh, S., Den Hengel, A.: Memorizing normality to detect anomaly: Memory-augmented deep autoencoder for unsupervised anomaly detection. In: *Proceedings of IEEE International Conference on Computer Vision*. pp. 1705–1714. IEEE (2019)

31. Gu, A., Dao, T., Ermon, S., Rudra, A., Ré, C.: Hippo: Recurrent memory with optimal polynomial projections. *Advances in neural information processing systems* 33, 1474–1487 (2020)
32. Guo, C., Wang, H., Xia, Y., Feng, G.: Learning appearance-motion synergy via memory-guided event prediction for video anomaly detection. *IEEE Transactions on Circuits and Systems for Video Technology* (2023)
33. Hirschorn, O., Avidan, S.: Normalizing flows for human pose anomaly detection. In: *Proceedings of the IEEE/CVF International Conference on Computer Vision*. pp. 13545–13554 (2023)
34. Huang, X., Hu, Y., Luo, X., Han, J., Zhang, B., Cao, X.: Boosting variational inference with margin learning for few-shot scene-adaptive anomaly detection. *IEEE Transactions on Circuits and Systems for Video Technology* (2022)
35. Ionescu, R.T., Khan, F.S., Georgescu, M.I., Shao, L.: Object-centric auto-encoders and dummy anomalies for abnormal event detection in video. In: *Proceedings of the IEEE/CVF Conference on Computer Vision and Pattern Recognition*. pp. 7842–7851 (2019)
36. Kim, S., Choi, K., Choi, H.S., Lee, B., Yoon, S.: Towards a rigorous evaluation of time-series anomaly detection. In: *Proceedings of the AAAI Conference on Artificial Intelligence*. vol. 36, pp. 7194–7201. AAAI Press (2022)
37. Li, B., Leroux, S., Simoens, P.: Decoupled appearance and motion learning for efficient anomaly detection in surveillance video. *Computer Vision and Image Understanding* 210, 103249 (2021)
38. Li, G., Cai, G., Zeng, X., Zhao, R.: Scale-aware spatio-temporal relation learning for video anomaly detection. In: *European Conference on Computer Vision*. pp. 333–350. Springer (2022)
39. Li, J., Huang, Q., Du, Y., Zhen, X., Chen, S., Shao, L.: Variational abnormal behavior detection with motion consistency. *IEEE Transactions on Image Processing* 31, 275–286 (2021)
40. Li, J., Xiong, C., Hoi, S.C.: Learning from noisy data with robust representation learning. In: *Proceedings of the IEEE/CVF International Conference on Computer Vision*. pp. 9485–9494 (2021)
41. Li, N., Chang, F., Liu, C.: Spatial-temporal cascade autoencoder for video anomaly detection in crowded scenes. *IEEE Transactions on Multimedia* 23, 203–215 (2020)
42. Li, N., Chang, F., Liu, C.: A self-trained spatial graph convolutional network for unsupervised human-related anomalous event detection in complex scenes. *IEEE Transactions on Cognitive and Developmental Systems* (2022)
43. Li, S., Liu, F., Jiao, L.: Self-training multi-sequence learning with transformer for weakly supervised video anomaly detection. In: *Proceedings of the AAAI Conference on Artificial Intelligence*. vol. 24. AAAI Press (2022)
44. Li, X., Chen, M., Wang, Q.: Quantifying and detecting collective motion in crowd scenes. *IEEE Transactions on Image Processing* 29, 5571–5583 (2020)
45. Lim, S.K., Loo, Y., Tran, N.T., Cheung, N.M., Roig, G., Elovici, Y.: Doping: Generative data augmentation for unsupervised anomaly detection with gan. In: *2018 IEEE international conference on data mining (ICDM)*. pp. 1122–1127. IEEE (2018)
46. Lin, X., Chen, Y., Li, G., Yu, Y.: A causal inference look at unsupervised video anomaly

- detection. In: Proceedings of the Thirty-sixth AAAI Conference on Artificial Intelligence. AAAI Press (2022)
47. Liu, B., Tan, P.N., Zhou, J.: Unsupervised anomaly detection by robust density estimation. In: Proceedings of the AAAI Conference on Artificial Intelligence. AAAI Press (2022)
 48. Liu, W., Luo, W., Lian, D., Gao, S.: Future frame prediction for anomaly detection—a new baseline. In: Proceedings of the IEEE Conference on Computer Vision and Pattern Recognition. pp. 6536–6545. IEEE (2018)
 49. Liu, W., Chang, H., Ma, B., Shan, S., Chen, X.: Diversity-measurable anomaly detection. In: Proceedings of the IEEE/CVF Conference on Computer Vision and Pattern Recognition. pp. 12147–12156 (2023)
 50. Liu, Y., Yang, D., Wang, Y., Liu, J., Liu, J., Boukerche, A., Sun, P., Song, L.: Generalized video anomaly event detection: Systematic taxonomy and comparison of deep models. *ACM Computing Surveys* (2023)
 51. Liu, Y., Cadei, R., Schweizer, J., Bahmani, S., Alahi, A.: Towards robust and adaptive motion forecasting: A causal representation perspective. In: Proceedings of the IEEE/CVF Conference on Computer Vision and Pattern Recognition. pp. 17081–17092. IEEE (2022)
 52. Liu, Z., Nie, Y., Long, C., Zhang, Q., Li, G.: A hybrid video anomaly detection framework via memory-augmented flow reconstruction and flow-guided frame prediction. In: Proceedings of the IEEE/CVF international conference on computer vision. pp. 13588–13597 (2021)
 53. Liu, Z., Wu, X.M., Zheng, D., Lin, K.Y., Zheng, W.S.: Generating anomalies for video anomaly detection with prompt-based feature mapping. In: Proceedings of the IEEE/CVF Conference on Computer Vision and Pattern Recognition. pp. 24500–24510 (2023)
 54. Lu, C., Shi, J., Jia, J.: Abnormal event detection at 150 fps in matlab. In: Proceedings of the IEEE International Conference on Computer Vision. pp. 2720–2727. IEEE (2013)
 55. Lu, Y., Yu, F., Reddy, M.K.K., Wang, Y.: Few-shot scene-adaptive anomaly detection. In: Computer Vision—ECCV 2020: 16th European Conference, Glasgow, UK, August 23–28, 2020, Proceedings, Part V 16. pp. 125–141. Springer (2020)
 56. Lu, Y., Cao, C., Zhang, Y., Zhang, Y.: Learnable locality-sensitive hashing for video anomaly detection. *IEEE Transactions on Circuits and Systems for Video Technology* 33(2), 963–976 (2022)
 57. Luo, W., Liu, W., Gao, S.: A revisit of sparse coding based anomaly detection in stacked rnn framework. In: Proceedings of IEEE International Conference on Computer Vision. pp. 341–349. IEEE (2017)
 58. Luo, W., Liu, W., Gao, S.: Normal graph: Spatial temporal graph convolutional networks based prediction network for skeleton based video anomaly detection. *Neurocomputing* 444, 332–337 (2021)
 59. Luo, W., Liu, W., Lian, D., Gao, S.: Future frame prediction network for video anomaly detection. *IEEE transactions on pattern analysis and machine intelligence* 44(11), 7505–7520 (2021)
 60. Luo, W., Liu, W., Lian, D., Tang, J., Duan, L., Peng, X., Gao, S.: Video anomaly detection with sparse coding inspired deep neural networks. *IEEE transactions on pattern analysis and machine intelligence* 43(3), 1070–1084 (2019)
 61. Lv, H., Chen, C., Cui, Z., Xu, C., Li, Y., Yang, J.: Learning normal dynamics in videos with meta prototype network. *arXiv preprint arXiv:2104.06689* (2021)

62. Lv, H., Yue, Z., Sun, Q., Luo, B., Cui, Z., Zhang, H.: Unbiased multiple instance learning for weakly supervised video anomaly detection. In: Proceedings of the IEEE/CVF Conference on Computer Vision and Pattern Recognition. pp. 8022–8031 (2023)
63. Madan, N., Farkhondeh, A., Nasrollahi, K., Escalera, S., Moeslund, T.B.: Temporal cues from socially unacceptable trajectories for anomaly detection. In: Proceedings of the IEEE/CVF International Conference on Computer Vision. pp. 2150–2158 (2021)
64. Madan, N., Ristea, N.C., Ionescu, R.T., Nasrollahi, K., Khan, F.S., Moeslund, T.B., Shah, M.: Self-supervised masked convolutional transformer block for anomaly detection. IEEE Transactions on Pattern Analysis and Machine Intelligence (2023)
65. Markovitz, A., Sharir, G., Friedman, I., Zelnik-Manor, L., Avidan, S.: Graph embedded pose clustering for anomaly detection. In: Proceedings of the IEEE/CVF Conference on Computer Vision and Pattern Recognition. pp. 10539–10547. IEEE (2020)
66. Morais, R., Le, V., Tran, T., Saha, B., Mansour, M., Venkatesh, S.: Learning regularity in skeleton trajectories for anomaly detection in videos. In: Proceedings of the IEEE Conference on Computer Vision and Pattern Recognition. pp. 11996–12004. IEEE (2019)
67. Nguyen, T.N., Meunier, J.: Anomaly detection in video sequence with appearance motion correspondence. In: Proceedings of the IEEE International Conference on Computer Vision. pp. 1273–1283. IEEE (2019)
68. Panariello, A., Porrello, A., Calderara, S., Cucchiara, R.: Consistency-based self-supervised learning for temporal anomaly localization. In: European Conference on Computer Vision. pp. 338–349. Springer (2022)
69. Pang, G., Yan, C., Shen, C., Hengel, A.v.d., Bai, X.: Self-trained deep ordinal regression for end-to-end video anomaly detection. In: Proceedings of the IEEE/CVF Conference on Computer Vision and Pattern Recognition. pp. 12173–12182. IEEE (2020)
70. Park, H., Noh, J., Ham, B.: Learning memory-guided normality for anomaly detection. In: Proceedings of the IEEE/CVF Conference on Computer Vision and Pattern Recognition. pp. 14372–14381. IEEE (2020)
71. Perini, L., Vercruyssen, V., Davis, J.: Transferring the contamination factor between anomaly detection domains by shape similarity. In: Proceedings of the AAAI Conference on Artificial Intelligence. vol. 36, pp. 4128–4136. AAAI Press (2022)
72. Purwanto, D., Chen, Y.T., Fang, W.H.: Dance with self-attention: A new look of conditional random fields on anomaly detection in videos. In: Proceedings of the IEEE/CVF International Conference on Computer Vision. pp. 173–183 (2021)
73. Pytorch, A.D.I.: Pytorch (2018)
74. Radford, A., Kim, J.W., Hallacy, C., Ramesh, A., Goh, G., Agarwal, S., Sastry, G., Askell, A., Mishkin, P., Clark, J., et al.: Learning transferable visual models from natural language supervision. In: International conference on machine learning. pp. 8748–8763. PMLR (2021)
75. Ramachandra, B., Jones, M.J., Vatsavai, R.R.: A survey of single-scene video anomaly detection. IEEE transactions on pattern analysis and machine intelligence 44(5), 2293–2312 (2020)
76. Reiss, T., Hoshen, Y.: Attribute-based representations for accurate and interpretable video anomaly detection. arXiv preprint arXiv:2212.00789 (2022)
77. Ren, S., He, K., Girshick, R., Sun, J.: Faster r-cnn: Towards real-time object detection with region proposal networks. Advances in neural information processing systems 28 (2015)

78. Ristea, N.C., Madan, N., Ionescu, R.T., Nasrollahi, K., Khan, F.S., Moeslund, T.B., Shah, M.: Self-supervised predictive convolutional attentive block for anomaly detection. *arXiv preprint arXiv:2111.09099* (2021)
79. Sabokrou, M., Khalooei, M., Fathy, M., Adeli, E.: Adversarially learned one-class classifier for novelty detection. In: *Proceedings of the IEEE Conference on Computer Vision and Pattern Recognition*. pp. 3379–3388. IEEE (2018)
80. Sapkota, H., Yu, Q.: Bayesian nonparametric submodular video partition for robust anomaly detection. In: *Proceedings of the IEEE/CVF Conference on Computer Vision and Pattern Recognition*. pp. 3212–3221 (2022)
81. Sato, F., Hachiuma, R., Sekii, T.: Prompt-guided zero-shot anomaly action recognition using pretrained deep skeleton features. In: *Proceedings of the IEEE/CVF Conference on Computer Vision and Pattern Recognition*. pp. 6471–6480 (2023)
82. Selvaraju, R.R., Cogswell, M., Das, A., Vedantam, R., Parikh, D., Batra, D.: Grad-cam: Visual explanations from deep networks via gradient-based localization. In: *Proceedings of the IEEE international conference on computer vision*. pp. 618–626 (2017)
83. Shi, C., Sun, C., Wu, Y., Jia, Y.: Video anomaly detection via sequentially learning multiple pretext tasks. In: *Proceedings of the IEEE/CVF International Conference on Computer Vision*. pp. 10330–10340 (2023)
84. Shi, H., Wang, L., Zhou, S., Hua, G., Tang, W.: Abnormal ratios guided multiphase self-training for weakly-supervised video anomaly detection. *IEEE Transactions on Multimedia* (2023)
85. Singh, A., Jones, M.J., Learned-Miller, E.G.: Eval: Explainable video anomaly localization. In: *Proceedings of the IEEE/CVF Conference on Computer Vision and Pattern Recognition*. pp. 18717–18726 (2023)
86. Stergiou, A., De Weerd, B., Deligiannis, N.: Holistic representation learning for multitask trajectory anomaly detection. In: *Proceedings of the IEEE/CVF Winter Conference on Applications of Computer Vision*. pp. 6729–6739 (2024)
87. Sultani, W., Chen, C., Shah, M.: Real-world anomaly detection in surveillance videos. In: *Proceedings of the IEEE conference on computer vision and pattern recognition*. pp. 6479–6488 (2018)
88. Sultani, W., Chen, C., Shah, M.: Real-world anomaly detection in surveillance videos. In: *Proceedings of the IEEE Conference on Computer Vision and Pattern Recognition*. p. 6479–6488 (2018)
89. Sun, C., Jia, Y., Hu, Y., Wu, Y.: Scene-aware context reasoning for unsupervised abnormal event detection in videos. In: *Proceedings of the 28th ACM International Conference on Multimedia*. pp. 184–192 (2020)
90. Sun, S., Gong, X.: Hierarchical semantic contrast for scene-aware video anomaly detection. In: *Proceedings of the IEEE/CVF Conference on Computer Vision and Pattern Recognition*. pp. 22846–22856 (2023)
91. Tian, Y., Pang, G., Chen, Y., Singh, R., Verjans, J.W., Carneiro, G.: Weakly-supervised video anomaly detection with robust temporal feature magnitude learning. In: *Proceedings of the IEEE/CVF international conference on computer vision*. pp. 4975–4986 (2021)
92. Todd, V.: Learn the oxford 3000™. *English Australia Journal* 31(2), 95–97 (2016)
93. Vaswani, A., Shazeer, N., Parmar, N., Uszkoreit, J., Jones, L., Gomez, A.N., Kaiser, Ł.,

- Polosukhin, I.: Attention is all you need. *Advances in neural information processing systems* 30 (2017)
94. Wang, G., Wang, Y., Qin, J., Zhang, D., Bao, X., Huang, D.: Video anomaly detection by solving decoupled spatio-temporal jigsaw puzzles. *arXiv preprint arXiv:2207.10172* (2022)
 95. Wang, S., Zeng, Y., Yu, G., Cheng, Z., Liu, X., Zhou, S., Zhu, E., Kloft, M., Yin, J., Liao, Q.: E3 outlier: a self-supervised framework for unsupervised deep outlier detection. *IEEE Transactions on Pattern Analysis and Machine Intelligence* 45(3), 2952–2969 (2022)
 96. Wang, X., Che, Z., Jiang, B., Xiao, N., Yang, K., Tang, J., Ye, J., Wang, J., Qi, Q.: Robust unsupervised video anomaly detection by multipath frame prediction. *IEEE transactions on neural networks and learning systems* 33(6), 2301–2312 (2021)
 97. Wu, J.C., Hsieh, H.Y., Chen, D.J., Fuh, C.S., Liu, T.L.: Self-supervised sparse representation for video anomaly detection. In: *European Conference on Computer Vision*. pp. 729–745. Springer (2022)
 98. Wu, P., Wang, W., Chang, F., Liu, C., Wang, B.: Dss-net: Dynamic self-supervised network for video anomaly detection. *IEEE Transactions on Multimedia* (2023)
 99. Wu, P., Liu, J.: Learning causal temporal relation and feature discrimination for anomaly detection. *IEEE Transactions on Image Processing* 30, 3513–3527 (2021)
 100. Wu, P., Liu, J., Shi, Y., Sun, Y., Shao, F., Wu, Z., Yang, Z.: Not only look, but also listen: Learning multimodal violence detection under weak supervision. In: *Computer Vision–ECCV 2020: 16th European Conference, Glasgow, UK, August 23–28, 2020, Proceedings, Part XXX* 16. pp. 322–339. Springer (2020)
 101. Yan, C., Zhang, S., Liu, Y., Pang, G., Wang, W.: Feature prediction diffusion model for video anomaly detection. In: *Proceedings of the IEEE/CVF International Conference on Computer Vision*. pp. 5527–5537 (2023)
 102. Yang, Z., Guo, Y., Wang, J., Huang, D., Bao, X., Wang, Y.: Towards video anomaly detection in the real world: A binarization embedded weakly-supervised network. *IEEE Transactions on Circuits and Systems for Video Technology* (2023)
 103. Yang, Z., Liu, J., Wu, Z., Wu, P., Liu, X.: Video event restoration based on keyframes for video anomaly detection. In: *Proceedings of the IEEE/CVF Conference on Computer Vision and Pattern Recognition*. pp. 14592–14601 (2023)
 104. Yang, Z., Wu, P., Liu, J., Liu, X.: Dynamic local aggregation network with adaptive clusterer for anomaly detection. In: *European Conference on Computer Vision*. pp. 404–421. Springer (2022)
 105. Yu, F., Zhang, M., Dong, H., Hu, S., Dong, B., Zhang, L.: Dast: Unsupervised domain adaptation in semantic segmentation based on discriminator attention and self-training. In: *Proceedings of the AAAI Conference on Artificial Intelligence*. vol. 35, pp. 10754–10762 (2021)
 106. Yu, G., Wang, S., Cai, Z., Liu, X., Xu, C., Wu, C.: Deep anomaly discovery from unlabeled videos via normality advantage and self-paced refinement. In: *Proceedings of the IEEE/CVF Conference on computer vision and pattern recognition*. pp. 13987–13998 (2022)
 107. Yu, J., Liu, J., Cheng, Y., Feng, R., Zhang, Y.: Modality-aware contrastive instance learning with self-distillation for weakly-supervised audio-visual violence detection. In: *Proceedings of the 30th ACM International Conference on Multimedia*. pp. 6278–6287 (2022)
 108. Yu, S., Zhao, Z., Fang, H., Deng, A., Su, H., Wang, D., Gan, W., Lu, C., Wu, W.: Regularity

- learning via explicit distribution modeling for skeletal video anomaly detection. *IEEE Transactions on Circuits and Systems for Video Technology* (2023)
109. Zaheer, M.Z., Mahmood, A., Khan, M.H., Segu, M., Yu, F., Lee, S.I.: Generative cooperative learning for unsupervised video anomaly detection. In: *Proceedings of the IEEE/CVF conference on computer vision and pattern recognition*. pp. 14744–14754 (2022)
 110. Zaheer, M.Z., Lee, J.h., Astrid, M., Lee, S.I.: Old is gold: Redefining the adversarially learned one-class classifier training paradigm. In: *Proceedings of the IEEE/CVF Conference on Computer Vision and Pattern Recognition*. pp. 14183–14193. IEEE (2020)
 111. Zaheer, M.Z., Lee, J.H., Mahmood, A., Astrid, M., Lee, S.I.: Stabilizing adversarially learned one-class novelty detection using pseudo anomalies. *IEEE Transactions on Image Processing* 31, 5963–5975 (2022)
 112. Zaheer, M.Z., Mahmood, A., Astrid, M., Lee, S.I.: Claws: Clustering assisted weakly supervised learning with normalcy suppression for anomalous event detection. In: *European Conference on Computer Vision*. pp. 358–376. Springer (2020)
 113. Zanella, L., Liberatori, B., Menapace, W., Poiesi, F., Wang, Y., Ricci, E.: Delving into clip latent space for video anomaly recognition. *arXiv preprint arXiv:2310.02835* (2023)
 114. Zeng, X., Jiang, Y., Ding, W., Li, H., Hao, Y., Qiu, Z.: A hierarchical spatio-temporal graph convolutional neural network for anomaly detection in videos. *IEEE Transactions on Circuits and Systems for Video Technology* (2021)
 115. Zhang, C., Li, G., Qi, Y., Wang, S., Qing, L., Huang, Q., Yang, M.H.: Exploiting completeness and uncertainty of pseudo labels for weakly supervised video anomaly detection. In: *Proceedings of the IEEE/CVF Conference on Computer Vision and Pattern Recognition*. pp. 16271–16280 (2023)
 116. Zhang, S., Gong, M., Xie, Y., Qin, A.K., Li, H., Gao, Y., Ong, Y.S.: Influence-aware attention networks for anomaly detection in surveillance videos. *IEEE Transactions on Circuits and Systems for Video Technology* 32(8), 5427–5437 (2022)
 117. Zhang, X., Fang, J., Yang, B., Chen, S., Li, B.: Hybrid attention and motion constraint for anomaly detection in crowded scenes. *IEEE Transactions on Circuits and Systems for Video Technology* (2022)
 118. Zhang, Y., Nie, X., He, R., Chen, M., Yin, Y.: Normality learning in multispace for video anomaly detection. *IEEE Transactions on Circuits and Systems for Video Technology* 31(9), 3694–3706 (2020)
 119. Zhang, Y.X., Meng, H., Cao, X.M., Zhou, Z., Yang, M., Adhikary, A.R.: Interpreting vulnerabilities of multi-instance learning to adversarial perturbations. *Pattern Recognition* p. 109725 (2023)
 120. Zhong, J.X., Li, N., Kong, W., Shan Liu, T.H.L., Li, G.: Graph convolutional label noise cleaner: Train a plug-and-play action classifier for anomaly detection. In: *Proceedings of the IEEE Conference on Computer Vision and Pattern Recognition*. p. 1237–1246. IEEE (2019)
 121. Zhong, Y., Yang, J., Zhang, P., Li, C., Codella, N., Li, L.H., Zhou, L., Dai, X., Yuan, L., Li, Y., et al.: Regionclip: Region-based language-image pretraining. In: *Proceedings of the IEEE/CVF Conference on Computer Vision and Pattern Recognition*. pp. 16793–16803 (2022)
 122. Zhong, Y., Chen, X., Hu, Y., Tang, P., Ren, F.: Bidirectional spatio-temporal feature learning with multiscale evaluation for video anomaly detection. *IEEE Transactions on Circuits and*

Systems for Video Technology 32(12), 8285–8296 (2022)

123. Zhou, H., Yu, J., Yang, W.: Dual memory units with uncertainty regulation for weakly supervised video anomaly detection. arXiv preprint arXiv:2302.05160 (2023)
124. Zhu, Y., Bao, W., Yu, Q.: Towards open set video anomaly detection. In: European Conference on Computer Vision. pp. 395–412. Springer (2022)